

Hybrid Transcutaneous Energy Transfer System for Medical Implants

Ehsan Jmashidpour^{1,2}, Guy Sturtzer^{1,3}, Michel Kam³, Jérôme KLEIN³, Luc Hebrard¹, Wilfried Uhring¹

1- ICube laboratory - UMR 7357, Strasbourg, France

2- School of Engineering ECAM Strasbourg-Europe, Strasbourg, France

3- Institut National des Sciences Appliquées (INSA) de Strasbourg, Strasbourg, France

Email: ehsan.jmashidpour@ecam-strasbourg.eu

Abstract—Medical Implants need batteries to sustain reliable power for the circuits. Battery replacement is usually inconvenient (or impossible) to the user experience. Wireless power transfer (WPT) could be the solution for this problem. This paper proposes a Transcutaneous Energy Transfer (TET) system with two parallel energy sources. A magnetic link and an optical link are used to energy transfer. An MPPT algorithm is applied to extract the maximum power of the optical link. An Ultra-Capacitor (UC) is preferred to the battery because of its rapid charge-discharge cycle. A few experimental tests are performed to validate the proposed TET system.

Keywords— Wireless power transfer; Transcutaneous Energy Transfer; photovoltaic; Medical Implants.

I. INTRODUCTION

In recent years, progress in semiconductor technology has led to miniature, wireless and low-power biomedical implants such as artificial organ, physiological signal sensing and neural recording and stimulation. There are many advantages in these new implants that can greatly improve the quality of the patient's life such as lower discomfort, lower infection risk and free activity [1], [2]. However, supplying the implants is remained as one of the major challenges because of the limited lifetime of their integrated battery. Recently Transcutaneous Energy Transfer (TET) systems have been widely used to either directly power up the implants or recharge their battery without any physical connection between the transmitter and receiver sides [2]. In the past decade, inductive links, optical links and ultrasonic powering have been the most attractive and efficient method among the several methods for TET systems over short distances that are reported in the scientific literature [3], [4], [5], [6].

In this paper, two different methods of Wireless Power Transmission (WPT) are used in order to supply a chip placed under the human skin that has inductive and optical links. These methods are more efficient than other wireless energy transfer methods [5], [6]. Based on the reported results for different applications, the human skin has no impact on the magnetic field that is used to transfer the energy from outside to the inside of the body (in a standard range of the frequencies). However, for the optical method, there are some limitations such as scattering and absorption of photons by the different layers of the human body [7], [8].

For the TET systems which are used in the medical application, a highest efficiency must be considered for the system design, in order to avoid all the uncontrolled tissue heating in sensitive human body areas [9]. There are two European standards for the electromagnetics filed and the lighting limitation, the European standard UE 1999/519/CE and UE 2006/25/CE that have been considered respectively.

In this paper, a transcutaneous energy transfer system is proposed. Two main energy sources are considered for the

proposed system: an inductive link and an optical link. The both sources can supply the system in parallel. In the next section, the TET system is presented. In section III the system modeling and calculation is detailed. The experimental results are discussed in section IV. A conclusion is given in section V.

II. SYSTEMS DESCRIPTION

Fig. 1 presents a schematic of the proposed TET system. There are two important subsystems; the external (sender) unit and the implanted (receiver) unit. The implanted unit that is inside of the body consists of four parts:

1. Energy receiver (magnetic and optical receiver)
2. Storage element
3. DC-DC (or AC-DC) converter
4. Implants (loads)

The external units (senders) that are outside of the body, have two separated parts. For the magnetic method, an AC source will provide energy and transfer it via the magnetic link. However, for the optical method, the source of energy can be a Near Infra-Red (NIR) light source.

In the internal part after receiving energy, the voltage level will be adapted by the DC-DC and AC-DC converters for the storage element and the loads. In the next section, the two energy methods will be detailed.

III. SYSTEM MODELING AND CALCULATION

The first important constraint of the WPT system is the expected lifetime of the system due to its localization inside of the body. The second constraint is the batteries to sustain reliable power for the circuits. It is noticeable that battery replacement in many cases is not easy and it is usually inconvenient to the patients.

The studied system has to complete some constraints as follows:

1. Enough energy to supply a device that consumes 0.17 mWh for 12 hours.
2. An average voltage supplied by the chip of 1.7 volt dc.
3. A final size of 10mm² for an implantation under 2cm of

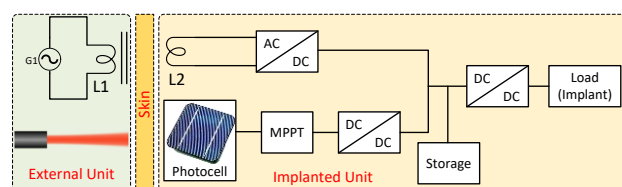


Fig. 1. Schematic of the studied transcutaneous energy transfer systems

skin.

In this section, the modeling and calculations of the storage element, magnetic link and optical link is expressed.

A. Storage element

One of the major problems in the design of the system is the storage element that it must satisfy the above constraints. As it mentioned before, a storage energy element must be able to supply the system with 0.17 mWh (17 mW for 1 second per hours) and it must hold on until the next charging time. The storage element will be charged every 12 hours. As 1 watt for 1 second is equal to a Joule, the storage element must have a capacity of 120 mJ to meet the specifications of the system.

There are two kinds of storage technologies that can be used in WPT systems: the battery and the Ultra-Capacitor (UC). The battery is already used in implants such as Pacemakers and is based on a chemical effect to store energy. This technology commonly uses lithium components. The UC stores electric charges in an electric field. Thanks to new technologies both of the storage elements can actually be small enough to be use in the medical implants. A lithium battery can store an important amount of energy but needs time to release it and needs a specific attention for the charge and discharge phases in order to limit the impact of the cycles on its lifetime. However, an UC can release an important amount of power quickly but cannot store as much as the battery. Furthermore, the UC is not as much corrosion sensitive as the chemical battery and it has a long lifetime without constraints on its charge or discharge. Moreover, an UC is refillable much faster than a battery.

The Table I shows the difference between a battery and an UC. Because of the lifetime needed for an implanted device, the limited number of components to reduce the consumption of the system and the need for a quick way of refilling, the UC is chosen as the storage element for the system.

To calculate the capacity of the UC we considered the

Table I Battery and UC characteristic

	Micro Lithium Lion battery	Super capacitor
Number of cycles	~1000 cycles	theoretically unlimited
Instant power	5 mW/cm ³	Up to 200 mW/cm ³
Storage	4.5 J/cm ³	200 mJ/cm ³
fulfillment constraints	Yes	No

system characteristic. The stored energy of an UC can be calculated as follows:

$$E_{uc} = \frac{1}{2} C V^2 \quad (1)$$

As it can be seen in (1), there are two parameters that control the store energy in an UC: its capacity and its terminal voltage. As it expressed before, the output voltage of the WPT system has to regulated on 1.7 V, which is not enough to have a large value of stored energy. Therefore, a DC-DC converter is needed to step up the voltage level at the terminal of the UC.

Regarding the available UCs, an UC with 1mF and 5.5 V is chosen for the studied system. Thus the stored energy is equal to 150 mJ as it calculated in equation (2). This amount of energy satisfies the 15 hours of autonomy for the system.

$$E_{uc} = \frac{1}{2} C V^2 = \frac{1}{2} \times 10 \times 10^{-3} \times 5.5^2 = 0.15 J \quad (2)$$

B. Magnetic link

Fig. 2 shows the equivalent electric circuit of the magnetic link. In order to have maximum transferred energy at secondary of the transformer, the follows equations for the load resistance (R_l) and the secondary capacitance (C_2) must be satisfied:

$$\begin{cases} R_l = \frac{\omega^2 L_2^2 + R_{b2}^2}{R_{b2}} \\ C_2 = \frac{L}{\omega^2 L_2^2 + R_{b2}^2} \end{cases} \quad (3)$$

In this condition the transferred power at the load terminal can be expressed as follows:

$$P_{out} = \frac{(M\omega I_1)^2}{4 \times R_{b2}} \quad (4)$$

Where ω is the frequency of the main source. It is noticeable that to remember that the magnetic field is limited by the European standard (UE 1999/519/CE). Therefore, the best parameter is the mutual inductance that can be determined to maximize the output power. On the other hand, due to the skin effect, the winding resistance (R_{b2}) will increase with increasing the frequency. Thus, a compromise will have to be considered between the frequency and the winding resistance.

Finally, a frequency of 150kHz is chosen for the magnetic link that makes it possible to limit the influence of the resistance of the secondary winding and to maximize the output power. The magnetic field will be limited to this frequency to 6.25 μ T. By fixing a number of turns $N_1 = 10$ for the primary coil, we can recalculate the current to guarantee compliance with the threshold:

$$\begin{aligned} I_1 &= \frac{H_d \times 2 \times (r_1^2 + 0^2)^{\frac{3}{2}}}{N_1 r_1^2} \\ &= \frac{6,25 \times 10^{-6} \times 2 \times (0,028^2 + 0^2)^{\frac{3}{2}}}{10 \times 0,028^2 \times 4 \times \pi \times 10^{-7}} \approx 28mA \end{aligned} \quad (5)$$

Fig. 3 shows the decrease of the magnetic field B which is simulated by the FEMM 4.2 software. We note that the maximum field of 6.25 μ T is guaranteed in contact with the patient. According to this result, it can be seen that the value of the field at distance of 2 cm (desired distance) is 3,4 μ T.

C. Magnetic field realization

It is noticeable that, in order to validate the inductive energy, transfer a prototype model scale 100 times greater than real size is realized and the distance between the two coils is 2 cm.

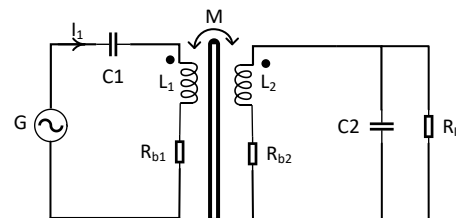


Fig. 2. Electric equivalent circuit of the magnetic link.

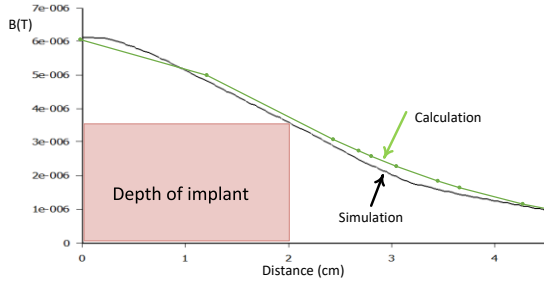


Fig. 3 Decrease of the field according to the distance

Normally, the geometry of the secondary winding will most often be imposed by the size of the medical implant. For a final model of 10 mm² (on the x100 scale), a maximum radius of 1.78 cm is proposed. The coil is made with a copper wire of 0.5 mm in diameter in order to limit its resistance for the high frequencies (around 1MHz). The number of laps was set at 10 laps. The measured radius of the inductor is 1.7 cm. The value of the inductance L_2 can be estimated by the formula of Harold A. Wheeler for a solenoid of finite length presented in equation (6). Or the approximation of Nagaoka expressed by equation (7) as follows:

$$L = \frac{10 \times \pi \times \mu_0 \times n_2^2 \times r_2^2}{9 \times r_2 + 10 \times l} \quad (6)$$

Where, r the radius of the inductor, N the number of turns, L the length of the solenoid.

$$L = \frac{0.0395 \times r_2^2 \times n_2^2 \times K}{l} \quad (7)$$

Where K is the coefficient of Nagaoka.

Table II summarizes the estimates with the two previous formulas as well as the measurement performed on the realized coil which it validates the estimation results.

To maximize the mutual inductance at a given distance the radius of the primary inductance must be $r_1 = \sqrt{2} \times d$. For a distance of $d=2\text{cm}$ the radius of the primary inductor is 2.8cm. Thus, the number of turns for the primary coil is fixed to 10 turns and then the estimated and measured inductance is also presented in TABLE II.

From the primary and secondary windings, the mutual

Table II Magnetic link parameters

	Harold A.Wheeler	Nagaoka	Measured
L_1 (μH)	10.4	11.1	10.76
L_2 (μH)	5.62	5.89	5.6
M (μH)	1.09	1,017	0,98
R_{b2} ($\text{m}\Omega$) at 150kHz	103	-	105
C_2 (nF)	199	-	197

inductance value can be estimated as follows:

$$M = \frac{\mu_0 n_1 r_1^2 n_2 r_2^2 \pi}{2 * \sqrt{(r_1^2 + d^2)^3}} = 1,09 \mu\text{H} \quad (8)$$

Fig. 4 shows the mutual as a function of the radius of the primary coil. It can be seen that the maximum value is around the radius of the primary winding determined previously, namely 2.8 cm. The mutual was measured at about 1 μH , the simulation gave 1.01 μH and a calculation 1.09 μH , a maximum deviation is about 10%. Fig. 5 shows the FEMM simulation result for the magnetic field B and the field lines generated by the primary coil to the secondary.

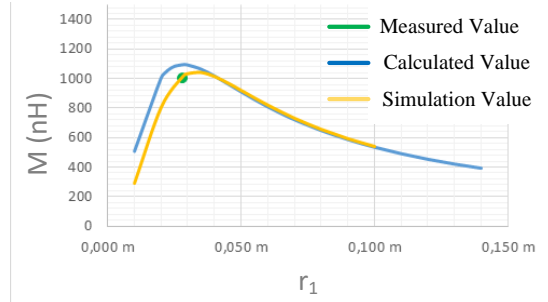


Fig. 4 Mutual Inductance as a Function of the Radius of the Primary Coil.

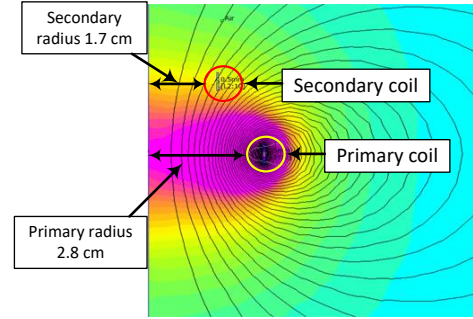


Fig.5 FEMM simulation of the magnetic field.

D. Optical link

A photovoltaic cell is used as a receiver for the optic link. There are several papers that studied PV cells modeling and its characteristic [10]. A model of moderate complexity for a solar cell was used as shown in Fig. 6. This model consists a current source in parallel with a diode and a series resistance R_s . In this model, the net current I can be expressed as follows:

$$I = I_{ph} - I_D = I_{ph} - I_0 \left(e^{\frac{q(V+IR_s)}{mkTc}} - 1 \right) \quad (1)$$

Where m is the idealizing factor, k is the Boltzmann's gas constant, T_c the absolute temperature of the cell, q the electron charge and I_0 is the dark saturation current, which is strongly depending on the temperature.

As it is shown in Fig. 1 the PV cell is connected to the system via a DC-DC converter. We have chosen a Boost converter that allows increasing the voltage at the terminal of the UC. In order to optimize the operation of a PV cell, it is important to follow the maximum power by an MPPT algorithm. The search for the optimal operating point of a PV by optimization techniques is relatively complex. In recent years, several MPPT methods have been published. Among these methods, we have chosen in this paper the P&O algorithm (Perturb and Observe) which is one of the most used methods [10]. Fig. 7 illustrates the principle of the P&O technique considered in this paper. Here, the operating voltage of the PV (V_{PV}) is perturbed by ΔV_{pv} in a given direction. Consequently, the power drawn from the PV also changes by ΔP_{pv} . If ΔP_{pv} is positive, it means that PPV increases and the operating point has moved toward the MPP. Therefore, the operating voltage must be further perturbed in the same direction. Otherwise, if the PPV decreases, the operating point has moved away from the MPP. Thus, the direction of the ΔV_{pv}

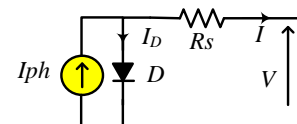


FIG. 6 Pv cell model

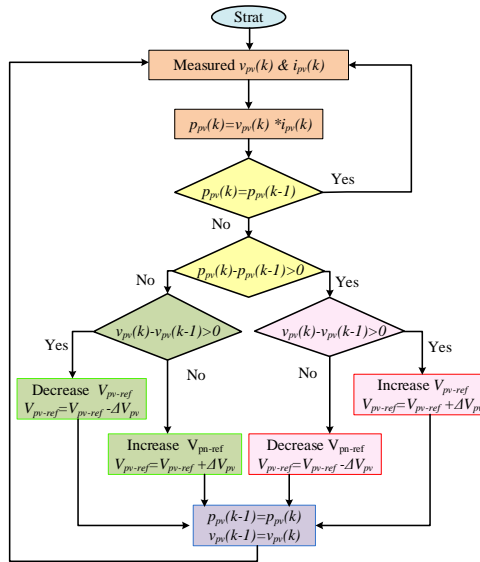
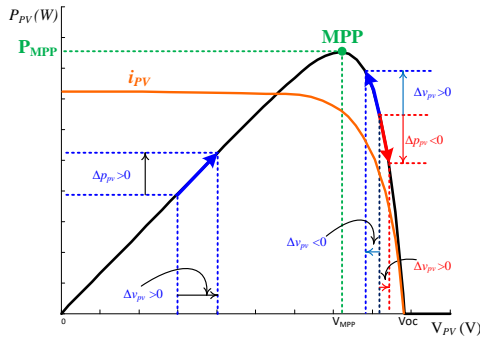


Fig. 7 P&O method for the MPPT.

must be reversed. more detail can be find in [10].

To use optical link as an energy source we have to study the light propagation in tissue. In this case, there are two phenomena must be considered: scattering and absorption, both of which are dependent on wavelength as well as the physical properties of the material [7]. In a few scientific literatures it can be found that penetration depths of a few mm are possible when using light in the NIR band (600-1300nm) with peaks occurring near 800nm [8]. It is now important to find a semiconductor material for which an efficient photodiode can be constructed to operate within this region. From the data presented in [11] that silicon photocells are ideal for operating in the NIR region around 800nm where the penetration depth in tissue is largest.

Therefore, in order to realize the optical link, a PV polycrystalline panel with dimensions of 140 * 100mm for a maximum power of 800mW is used. The MPPT algorithm it is implanted in an Intel Cyclone IV FPGA.

IV. EXPERIMENTAL RESULTS

In order to verify the validity of the proposed method, a few experimental tests are performed. Fig. 8 shows the UC voltage when the energy is transferred by the magnetic link. As it mentioned before, we need 120 mJ for the study system. Thus for an UC by 1 F the needed voltage that can be calculated from equation (1) is 490 mV. As Fig. 8 shows the UC terminals has 490 mV at around 180s.

To validate the optical link, the Boost converter which is controlled by the MPPT algorithm is working with a switching frequency of 20kHz. Fig. 9 shows the UC terminal voltage when the optical link is used to energy transfer.

These experimental results validate the energy transfer via the both magnetic and optical links wirelessly.

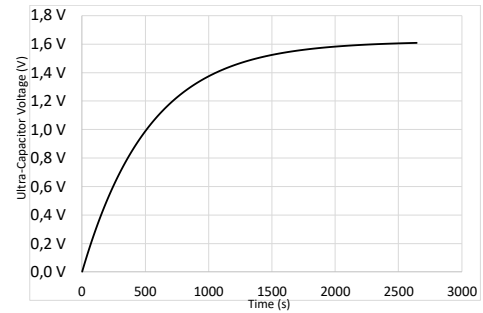


Fig. 8 Ultra-Capacitor voltage terminal charged by magnetic link.

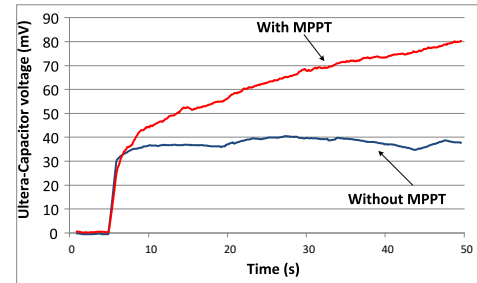


Fig. 9 Ultra-Capacitor voltage terminal charged by Optical link.

V. CONCLUSION

In this paper, a TET system with a hybrid primary source is presented. Two methods of wireless energy transfer are used to supply the receiver unit that is implanted in the human body. An ultra-capacitor is used as the storage element thanks to its rapid charge-recharge characteristic. A prototype model is realized to perform the experimental test that is needed to verify the validity of the proposed system.

REFERENCES

- [1] H. Liu, Q. Shao, and X. Fang, "Modeling and Optimization of Class-E Amplifier at Subnominal Condition in a Wireless Power Transfer System for Biomedical Implants," *IEEE Trans. Biomed. Circuits Syst.*, pp. 1–17, 2016.
- [2] H. S. Gougheri and M. Kiani, "Optimal wireless receiver structure for omnidirectional inductive power transmission to biomedical implants," *2016 38th Annu. Int. Conf. IEEE Eng. Med. Biol. Soc.*, no. 0, pp. 1975–1978, 2016.
- [3] I. Hashimoto, "Analysis of Low Leakage Magnetic Field Transcutaneous Energy Transfer for Ventricular Assist Devices," pp. 3–6, 2015.
- [4] C. Gong, D. Liu, Z. Miao, and H. Zhang, "A novel transcutaneous NFC uplink system symbiotic with inductive wireless power supply under ultra low coupling coefficient," *IEEE Biomed. Circuits Syst. Conf. Eng. Heal. Minds Able Bodies, BioCAS 2015 - Proc.*, 2015.
- [5] L. Mandache, A. Marinescu, and M. Iordache, "On Feasibility and Optimization of WiTricity Technology for Implantable Medical Devices," pp. 5–10, 2016.
- [6] S. Majerus, S. L. Garverick, and M. S. Damaser, "Wireless battery charge management for implantable pressure sensor," *2014 IEEE Dallas Circuits Syst. Conf. Enabling an Internet Things - From Sensors to Servers, DCAS 2014*, 2014.
- [7] B. J. Tromberg *et al.*, "Non-Invasive In Vivo Characterization of Breast Tumors Using Photon Migration Spectroscopy," *Neoplasia*, vol. 2, no. 1, pp. 26–40, 2000.
- [8] R. Srinivasan and M. Singh, "Laser backscattering and transillumination imaging of human tissues and their equivalent phantoms," *IEEE Trans. Biomed. Eng.*, vol. 50, no. 6, pp. 724–730, 2003.
- [9] J. Friedmann, F. Groedel, and R. Kennel, "Transcutaneous Energy Transmission for Medical Implants," pp. 1–6, 2014.
- [10] P. Ultra, C. Battery, E. Jamshidpour, P. Poure, and S. Saadate, "Energy Management and Control of a Stand-Alone," *Jordan J. Electr. Eng.*, vol. 2, no. 1, pp. 1–12, 2016.
- [11] S. M. Sze, "Semiconductor device physics and technology", *JOHN WILEY & SONS*

